Block Copolymer Micelles for Drug Delivery

Summary of dissertation for the degree of Master's in Chemical Engineering

Andreia Filipa Fidalgo de Sousa
Instituto Superior Técnico, Universidade de Lisboa, Portugal

ABSTRACT

Recently, several gold bisdithiolate complexes were studied aiming to find potential chemotherapeutic agents. However, their poor water solubility may hamper their action *in vivo*. Polymeric micelles offer the opportunity to solubilize hydrophobic drugs in their hydrophobic core and improve their bioavailability and their circulation time in blood. In this context, the goal of this project was to provide water solubility, prolonged availability, and an enhanced therapeutic index to the gold complex $[Au(cdc)_2]^-$ (where cdc = cyanodithioimido carbonate) loaded in polymeric micelles for drug-delivery. Given so, loaded micelles BCM-$[Au(cdc)_2]$ were synthesized and characterized. The BCM-$[Au(cdc)_2]$ were prepared with a loading efficiency of 64.59% and a loading content of 35.29 $mg_{[Au(cdc)2]-}/g_{BCM}$. The hydrodynamic diameter (D_h) and the zeta potential (Zp) of the micelles were determined by DLS and LDV, respectively. A D_h of 77.31 ± 27.00 nm and a low polidispersity index (PdI) of 0.18, were determined indicating the sample were homogenous and the micelles are good candidates for drug delivery. The zeta potential (-57.20 ± 12.10 mV) suggests high stability of the micelles. Cytotoxic activity studies against the ovarian A2780 cancer cells, have shown that $[Au(cdc)_2]$-loaded BCMs maintain relevant cytotoxic activity comparable to the cytotoxicity observed for the same concentration of gold complex. The micelles were radiolabeled with ^{111}In-oxine and ^{67}Ga-oxine in high radiochemical yield and purity (> 95%) affording ^{111}In-BCMs and ^{67}Ga-BCMs stable in PBS pH 7.4, at 37°C for at least 4 days. Biodistribution studies with ^{67}Ga-BCMs in healthy CD1 mice has shown prolonged circulation lifetime in the bloodstream.

KEYWORDS: polymeric micelles, drug delivery, loading content, radiolabeled, biodistribution

1 INTRODUCTION

Nanotechnology application in cancer treatment has the main objective of assuring drug delivery to their action sites in order to overcome the limitations of drugs and drawbacks that would hinder their required effectiveness and to maximize their pharmacological desired influence[1]. Nanocarraries, such as polymeric micelles, are used for drug delivery due to the reduction in toxicity while maintaining therapeutic effects and greater biocompatibility and safety[2]. These systems can overcome the drawbacks of therapeutic molecules and free drugs including non-selective activity for the targeted tissues, poor solubility, poor biodistribution and pharmacokinetics (PK), multi-drug resistance, dose-limiting toxicity and fast degradation in the harsh *in vivo* environment[3,4].

Polymeric micelles can be formed by natural polymers or complex synthetic copolymers that have a hydrophobic tail and mostly hydrophilic head – amphiphilic block copolymers. The selection of the polymer has an important role in the formation of micelles, and it is based on the characteristics of both hydrophilic and hydrophobic block polymers. The advantages of polymeric micelles are the following: (1) their ability to solubilize hydrophobic drugs or poorly water soluble within their core, thus enhancing their bioavailability; (2) their hydrophilic corona provides longer duration of circulation time inside the body, prevents a quick uptake of the formulation by RES and gives steric stability; (3)

their biocompatibility; and (4) their low toxicity[3,5–7].

The delivery of the drug is assured by the passive or active targeting. The first one exploits the pathophysiological and anatomical abnormalities of the tumour vasculature and uses the enhanced permeability and retention (EPR) effect[8] and the second one exploits the specific interactions (covalent or noncovalent) between the polymeric micelle and receptors or antigens on the target cell, which can also promote the internalization of nanocarriers trough receptor-mediated endocytosis.

In addition, polymeric micelles can be modified in order to include (1) surface modification with ligands to allow for selectivity targeting and the intracellular delivery of drugs, (2) modifications that allow micelles to answer to a number of extrinsic and intrinsic stimuli for "triggered" drug release at diseases sites, (3) modifications that incorporate a dye for imaging, and (4) modifications for longevity, which is important for the passive targeting. If the nanocarriers have two or more different modifications, that enable them to sequentially or simultaneously perform diagnostic and therapeutic functions, they are considered to be theranostic[3,8]. Hence, polymeric nanoparticles can also be used as pharmaceuticals for imaging in cancer diagnosis and/or therapy response evaluation

The incorporation of the imaging agent inside the polymeric nanoparticles, in addition to the drug agent, helps to monitor the localization and the pathway of these nanocarriers at the target site to assess, in a non-invasive way, the therapeutic response and the tumour physiology (in the case of cancer therapeutics)[9,10], so it is possible to verify the biodistribution of the nanoparticle in real time, even in *in vivo* studies[10,11]. Biodistribution is influenced by the interactions of the micelles with the organs, which are dependent on the physical and biochemical properties of the micelles and the characteristics of the organs[12]. Once the nanocarriers are injected, they are transferred by the bloodstream and distributed to peripheral organs, and simultaneously cleared by these. The clearance can be hepatic (through liver), renal (through kidneys), gastric (through gastrointestinal track) or mucociliary (through lungs), depending on the properties of the nanoparticles[12,13].

Recently, less explored gold(III) complexes based on bisdithiolenes have emerged as potential anticancer and antimicrobial agents[8,15,16]. However, these complexes have poor solubility in water, which poses some challenges regarding their *in vivo* administration even though it is not a limiting factor. The association of these compounds with nano-sized carriers such as micelles, could circumvent the solubility issue and reduce ligand displacement reactions with blood proteins[5]. With this in mind, the work presented herein focused on the use of polymeric micelles to encapsulate the gold complex $[Au(cdc)_2]^-$, in order to provide water solubility, prolonged availability, and consequently, enhance the therapeutic index of this gold complex, towards ovarian A2780 cancer cells.

2 EXPERIMENTAL PROCEDURES

UV-VIS Spectroscopy

Spectra of UV-VIS were obtained in a spectrophotometer Cary 60 UV/VIS (*Agilent-Technologies*) by using a quartz cuvette (QS High Precision Cell; 10mm (*Hellma® Analytics*)). The UV-VIS Spectroscopy was used to calculate the concentration of cdc inside the micelles after their preparation and disassembly.

High-Performance Liquid Chromatography (HPLC)

The analysis by HPLC were conducted in a modular equipment composed by a PerkinElmer Series 200 Pump and a PerkinElmer Series 200 UV/VIS Detector. The solvents used were acetonitrile and a TFA solution.

Preparation of Micelles

The micelles with the complex $[Au(cdc)_2]^-$ encapsulated (BCM-$Au(cdc)_2$) were synthesized by the thin-film hydration method[18]. For this method is necessary to use a round-bottom flask, so the film can be made after the removal of organic solvent.

The first step of the method was the dissolution of the polymer (50 mg), Me-PEG-*b*-PCL, and $[Au(cdc)_2]^-$ (2 – 8 mg) in $CHCl_3$ (4 mL), under constant stirring for 4 hours at

atmospheric pressure and room temperature (RT). Then, the solvent was slowly evaporated overnight under a flux of N_2 in order to form the $[Au(cdc)_2]^-$/Me-PEG-b-PCL thin-film, which was hydrated at 60 ºC with H_2O (or PBS) (1 mL) and stirred (low velocity) for 4 hours at RT. After the hydration, the solution was centrifuged for 10 minutes at 10000g and the supernatant was filtered by a SARTORIUS filter of 0.22 µm. The last step of this process was the lyophilization of the micelles.

Drug Loading Content and Efficiency

The drug loading, DL, was determined by UV-Vis Spectroscopy with reference to a standard calibration curve ($\mathrm{Abs} = 56.009 \times \mathrm{C} + 0.0247$, R= 0.997). In order to do this study, 2 – 4 mg of BCM-$Au(cdc)_2$ were dissolved in 1.0 mL of acetonitrile, vortex and centrifuged at 3000g for 10 minutes in order to precipitate the copolymer. After that, 600 µL of the supernatant were collected and analysed by UV-VIS spectroscopy.

Cells and Cell Culture Media

A2780 (cisplatin sensitive) ovarian cancer cells were purchased from Sigma-Aldrich. Cell media and media supplements were purchased from Gibco (Thermo Fisher Scientific). The cell lines were tested for mycoplasma using the LookOut® mycoplasma PCR Detection Kit.

Determination of Cytotoxic Activity

The cytotoxic activity of BCMs, $[Au(cdc)_2]^-$ and BCMs-$Au(cdc)_2$ was evaluated with the cisplatin-sensitive A2780 cell line. Cells were grown in RPMI medium supplemented with 10% FBS and maintained in a humidified incubator (Heraeus, Germany) with 5% CO_2. The MTT assay was used to assess the cellular viability as a function of redox potential, i.e., metabolic active cells convert the water-soluble MTT to an insoluble purple formazan. For the assays, cells (1-2×10^4 cells/200 µL medium) were seeded in 96-well plates and allowed to adhere for 24 h. Loaded BCMs (complex loading content of 3.56%) were diluted to prepare serial concentrations in the range 10 ng/mL-2g/mL a concentration that correspond to 10^{-7}-10^{-4} M of $[Au(cdc)_2]^-$. Unloaded BCMs were diluted in medium to prepare serial concentrations in the range 10 ng/mL-2 mg/mL. Loaded and unloaded micelles were added to the cells and incubated for 48 h at 37 ºC. At the end of the treatment, the medium was discarded and 200 µL of MTT solution in PBS (0.5 mg/mL) were added to each well. After 3 h at 37 °C, the medium was removed and DMSO (200 µL) was added to the cells to solubilize the formazan crystals. The percentage of cellular viability was assessed measuring the absorbance at 570 nm using a plate spectrophotometer (Power Wave Xs, Bio-Tek). The IC_{50} values were calculated using the GraphPad Prism software (version 5.0). Results are shown as the mean±SD of at least two experiments done with six replicates each.

Preparation of Radiolabeled micelles (^{111}In-BCM and ^{67}Ga-BCM)

The manipulation of all radioactive compounds was performed in a dedicated laboratory following the radiation protection rules. Activities were measured in ionization chamber (CRC-55tW by *CRC® - R Chamber)*, or in a gamma counter (Berthold, LB2111, Germany) for lower activities (< 37 kBq).

The first step was the reaction between 100 µL of oxine (8-hydroxychinolin, purity 99%, molecular weight 145.16, *E Merck Ag Darmstadt)* in ethanol (2 mg/mL) with 400 µL of sodium acetate buffer (pH 5, 0.4 M) and 100 µL of $^{111}InCl_3$ (111 MBq) in 0.01 M HCl. This reaction occurred at room temperature for 5 minutes and allowed the formation of ^{111}In-oxine. Afterwards, 500-700 µL of dichloromethane was used to extract the complex ^{111}In-oxine (soluble in DCM). The collected activity was measured on ionization chamber. The purity of the extracted complexes was evaluated by ITLC-SG using a mixture of $CHCl_3$/MeOH (90:10) as eluent (Rf (^{111}InCl3) = 0.0, Rf (^{111}In-oxine) = 0.9 - 1).

To the solution of ^{111}In-oxine in DCM, (1 – 1.5) mg of polymer (Me-PEG-b-PCL) was added and after that the solvent was evaporated under a flux of N_2. PBS (500 µL) was added to the thin-film, which resulted from the evaporation, and then the solution was put in the ultrasounds, under stirring, for 20 minutes at 35ºC.

After the formation, the radiolabeled micelles (^{111}In-BCM), were purified using Amicon ultra centrifugal filters (0.5 mL; MWCO

10 kDa). Briefly, the solution containing the ^{111}In-BCM was introduced in the selected Amicon filter and centrifuged during 10 minutes at 14000 rcf. Subsequently, 300 µL of PBS was added to the filter and a second centrifugation was performed using the same conditions. Finally, efficient recovery of the concentrated ^{111}In-BCM (retained species) was achieved by a convenient reverse spin step, after collecting the filtrate. Briefly, the Amicon filter containing the purified radiolabeled micelles was inverted in a new tube and one last centrifugation was performed during 2 minutes at 2000 rcf. Once again, the activity of the solution recovered from the filter (^{111}In-BCM) and the filtrate (^{111}In-oxine) were measured and the radiolabeling yield was calculated.

^{67}Ga-BCM were formed based on the protocol above, being the only difference the reaction for the formation ^{67}Ga-oxine lipophilic complex. This complex was formed by the reaction of 600 µL ^{67}Ga-citrate, which has the buffer incorporated, and 100 µL of the oxine solution. Also, the purity of the extracted ^{67}Ga-oxine was evaluated by ITLC-SG using a mixture of $CHCl_3$/MeOH (90:10) as eluent (Rf (^{67}Ga-citrate) = 0.0, Rf (^{67}Ga-oxine) = 0.9 -1).

IN VITRO STABILITY

To evaluate the *in vitro* stability of the radiolabeled micelles, ^{111}In-BCMs and ^{67}Ga-BCMs, were diluted in 0.1 M PBS pH 7.4 and incubated at 37 ºC. Aliquots taken at different time points (2, 4 and 6 days) were submitted to ultrafiltration using Amicon filters and the radioactivity of the filter and the filtrate were measured and used to calculate the activity retained in the micelles.

BIODISTRIBUTION

The biodistribution of ^{67}Ga-BCMs was evaluated in groups of CD1 mice (Charles river) with seven weeks, weighting between 25 and 28 g each. Animals were intravenously injected via the tail vein with 100 mL (4.6 – 5.0 MBq) of each preparation and a normal diet ad libitum was maintained. At 4 h and 24 h post-injection (p.i.) mice were sacrificed by cervical dislocation. The radioactivity in the sacrificed mouse and the radioactive administered dose were measured in a dose calibrator (Capintec CRC25R). The difference between the radioactivity in the injected and sacrificed mouse was assumed to be due to excretion. At sacrifice, a cardiac puncture was made in order to take blood samples. Then, tissue samples of the main organs were removed, weighted and counted in a gamma counter (LB2111, Berthold, Germany). The uptake in the tissues/organs was calculated and expressed as a percentage of the injected activity per gram (%I.A./ g)[18]. The performance of all the animal experiments was made accordantly with the guidelines for animal care and ethics for animal experiments outlined in the National and European Law.

3 RESULTS AND DISCUSSION

OPTIMISATION OF MICELLES LOADED WITH $[Au(cdc)_2]^-$

The first part of the optimisation for this process was made in order to decide which solvent to use for the dissolution of the polymer and the gold complex and for the hydration of the thin-film (Table 1). For all the studies the amount of $[Au(cdc)_2]^-$ and polymer was the same, 2mg and 25mg, respectively, in order to compare the results. In addition, the volume of solvent for the dissolution was between the range of 2-4 mL and for the hydration of the thin-film only 1 mL was used.

Table 1 – Formulations prepared for the optimization of micelles loaded with $[Au(cdc)_2]^-$.

	m $_{Au(cdc)_2}$ (mg)	**m $_{polymer}$ (mg)**	**Solvent for the dissolution of $Au(cdc)_2$**	**Solvent for the hydration of the thin-film**
AS1			DMF + DCM	PBS
AS2			ACN	H_2O
AS3	2	25	ACN	PBS
AS4			$CHCl_3$	H_2O
AS5			$CHCl_3$	PBS

The next step was the disassembly of the micelles, were 2 mg of micelles were used in order to know the amount of $[Au(cdc)_2]^-$ which was encapsulated. This analysis was done by UV-Vis spectroscopy at the wavelength of 303 nm, since the compound has the maximum of absorbance at that wavelength.

All the micelles studied have the gold complex encapsulated, with the exception of AS2, since all the spectra display a similar spectra profile as the spectrum obtained for the $[Au(cdc)_2]^-$ in acetonitrile, as shown in Figure 1.

A new absorption band appeared below 230 nm that was ascribed to the interaction with the medium.

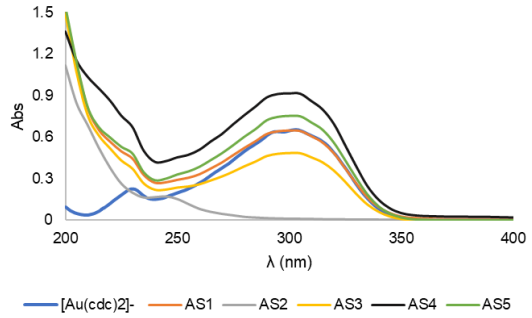

Figure 1 – Spectra of $[Au(cdc)_2]^-$ and the micelles prepared for the optimisation process.

Except for AS2, all the other micelles (AS1, AS3 – AS5) have gold compound encapsulated; however, AS3 has the lowest amount, which can mean that acetonitrile is not a good solvent for the dissolution of the copolymer and the gold compound, since in AS2 acetonitrile was also used. On the other hand, micelles in which the polymer and $[Au(cdc)_2]^-$ were dissolved with chloroform have the highest concentration of gold complex trapped in the micelles, so it is possible to conclude that $CHCl_3$ is a better solvent to prepare the micelles. In addition, the highest concentration is obtained using water during the hydration of the thin-film – AS4. To corroborate these findings, in Table 2 can be found the LC of these formulations. AS4 has the highest loading content (5.68 mg $_{Au(cdc)2]-}$ /g_{BCM}).

Table 2 – Results for the formulations AS1-AS5.

	m $_{[Au(cdc)2]-}$ (mg)	**m_{BCM} (mg)**	**LC (mg $_{Au(cdc)2]-}$ /g_{BCM})**
AS1	0.145	34.5	4.21
AS2	0.000	5.9	0.00
AS3	0.070	22.8	3.05
AS4	0.096	16.9	5.68
AS5	0.118	22.4	5.27

In addition, studies in HPLC were conducted, in order to observe if there was any type of degradation of the compound when encapsulated. In order to verify this, the retention times (t_r) – time from the injection of the sample to the time of the elution of the compound[20] – were analysed. The t_r of $[Au(cdc)_2]^-$ is 12.11 minutes. In comparison, the retention time of AS4 is 12.20 minutes and since the profile of the two chromatograms is similar, it is possible to conclude that the compound was encapsulated, and it did not suffer any type of degradation (Figure 2).

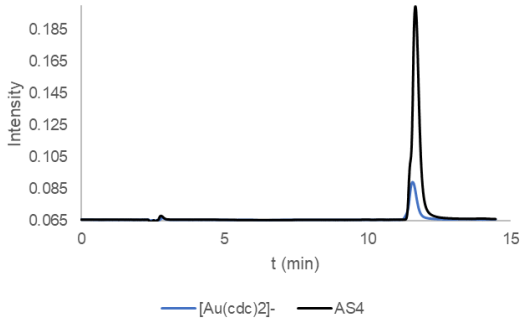

Figure 2 – Chromatogram of $[Au(cdc)_2]^-$ *vs* AS4.

For the second part of the optimisation, it was necessary to study the amount of $[Au(cdc)_2]^-$ needed in order to have the highest drug loading. For this, the amount of polymer was constant, 50 mg, and the amount of $[Au(cdc)_2]^-$ varied between 1-8 mg. Table 3 resumes this optimisation.

Table 3 – Values of the second optimisation.

	$m_{[Au(cdc)2]-}$ (mg)	**LE (%)**	**LC (mg_{cdc}/g_{BCM})**
AS6	2	64.59	35.29
AS7	4	7.81	8.47
AS8	8	3.34	7.11
AS9	1	65.68	24.25

AS6 and AS9 have the major LC and LE when compared to the other two formulations, so it is possible to conclude that the drug loading content and efficiency are higher for lower quantities of $[Au(cdc)_2]^-$ (for a constant value of copolymer). In order to choose the best formulation of BCMs-$Au(cdc)_2$, the LC of AS6 and AS9 were compared. As it possible to verify in Table 3, AS6 has the higher value (35.29 *vs* 24.25 mg $_{Au(cdc)2]-}$ /g_{BCM}), so the optimal amount of the gold compound is 2 mg *vs* 50 mg of Me-PEG-b-PCL.

Afterwards, the results were compared to the ones obtained for the study of auranofin-

loaded nanoparticles[21], since auranofin is a gold compound in study for the treatment of bacterial infections, as $[Au(cdc)_2]^-$ [19].The achieved drug loading content for auranofin was in the range of 1.8 – 6.2 mg[21] in comparison to 35.29 mg of $[Au(cdc)_2]^-$ per gram of micelles in formulation AS6. These results show a drug loading content higher in the $[Au(cdc)_2]^-$ loaded micelles, indicating that $[Au(cdc)_2]^-$ is encapsulated more efficiently using the optimized formulation. This is a very important achievement since a lower quantity of loaded micelles may be used to deliver the same amount of gold complex. In addition, in the experiments with the auranofin they used a different polymer – the PGLA (poly(lactic-co-glycolic acid) – instead of the Me-PEG-b-PCL. Also, the quantities used were different, in the study with auranofin they used 10-15 mg of the compound and 200mg of PLGA and in this experiment it was used 2 mg of $[Au(cdc)_2]^-$ and 50 mg of Me-PEG-b-PCL. In order to have a good comparison the experiment should have been done with the same conditions as in the one for auranofin.

Size and Zeta Potential of Micelles

This study was conducted on the following formulations of micelles: AS1, AS4 and AS6. These micelles were chosen based on the higher loading content, previously mentioned.

Micelles were formed, since the diameter obtained is in the range of 10 – 100 nm[22]. Also, based on the values, which are the average of the three measurements, present on Table 4, it is possible to conclude that the hydrodynamic diameter (d_h) is higher for micelles with a higher loading content. In addition, the micelles with the bigger d_h are the ones where it was used 50 mg of polymer instead of 25 mg.

The polydispersity index (PdI), which indicates the quality of the size of micelles[23], was also studied and can vary between 0.0 and 1.0. In this specific case, drug delivery applications using lipid-based nanocarriers, the sample is considered to be homogenous, and as a consequence acceptable, for values of 0.3 or below[23] , so the micelles acceptable for drug delivery are the ones from the batch AS4 and AS6 and between this two, AS6 has the best value of PdI, i.e. has the lowest value indicating that the sample is more homogenous than AS4.

Table 4 – Hydrodynamic diameter and Zeta Potential of micelles.

	d_h (nm)	PdI	Z_p (mV)
AS1	50.96 ± 20.06	0.42	-63.03 ± 9.75
AS4	70.56 ± 35.49	0.30	-51.10 ± 9.92
AS6	77.31 ± 27.00	0.18	-57.20 ± 12.10

Zeta potential is a standard characterization technique that evaluates nanoparticles surface charge which can provide understanding into circulation times, nanoparticle stability, biocompatibility, particle cell permeability and protein interactions[24]. Absolute Z_p values >30 mV are required for full electrostatic stabilization; potentials between 5 and 15 mV are in the region of limited flocculation; and for values lower than 3 mV exists the tendency to occur maximum flocculation. Hence, particle aggregation is less expected to occur for charged particles (high Z_p) due to electric repulsion. In this study, the Z_p analysis (Table 4) enables us to conclude that, based on absolute high Z_p alues (>50 mV), the micelles should not have tendency to aggregate. In addition, all the micelles formed are anionic, i.e. the surface is negatively charged, which leads to a higher rate of clearance from the blood[25]. This can be a problem since micelles have to remain in circulation for longer intervals without being taken up by the MPS in order to enter the tumour tissues through the EPR effect.

Antiproliferative Activity

In a previous publication it was demonstrated that the gold complex $[Au(cdc)_2]^-$ displayed a remarkable antiproliferative activity in the ovarian cancer cell line A2780[19]. Using the colorimetric MTT assay (MTT= (3-(4,5-dimethylthiazol-2-yl)-2,5-diphenyltetrazolium bromide)) to assess the cellular viability, the IC_{50} value – the concentration of complex required for 50% inhibition – was calculated after 48 hours treatment. However, as previously referred, this gold complex is water insoluble, one disadvantage for biological applications. Encapsulation of this gold complex into the block copolymer micelles was used to achieve water solubilization aiming to maintain the referred antiproliferative activity. In order to evaluate if the BCMs-$Au(cdc)_2$ are still active against the ovarian A2780 cancer cells, the MTT assay was used to compare the activity of the loaded and the unloaded BCM. Results shown in Figure 3 demonstrate that the dose response curves obtained with $[Au(cdc)_2]^-$ and

BCMs-Au(cdc)$_2$ do not differ, being the IC_{50} of 1.0 and 1.8 µM for $[Au(cdc)_2]^-$ and BCMs-Au(cdc)$_2$, respectively.

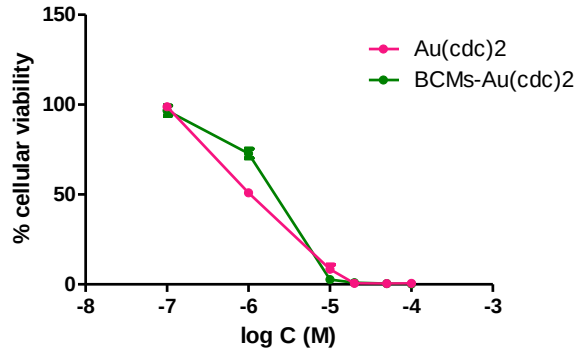

Figure 3 – Dose-response curves found for $[Au(cdc)_2]^-$ and BCMs-Au(cdc)$_2$, using the MTT assay. The IC_{50} values were calculated using the GraphPad Prism software (version 5.0). Results shown are the mean±SD of at least two experiments done with six replicates each.

The cytotoxicity of the unloaded BCMs was also evaluated by the MTT assay. It is possible to observe in Figure 4 that only for concentrations higher than 2 mg/mL, there was *ca*. 30% loss of cellular viability. This concentration of unloaded BCMs is equivalent to that used in BCMs-Au(cdc)$_2$ for the higher concentration of $[Au(cdc)_2]^-$ (100 µM).

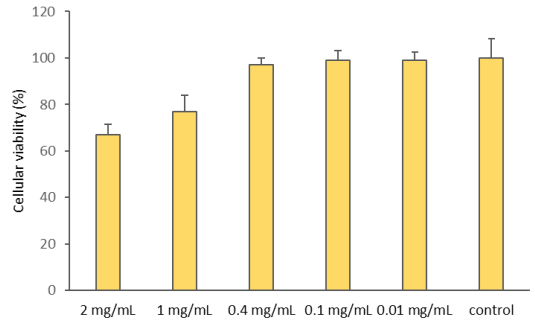

Figure 4 – Cellular viability of A2780 cells after incubation with BCMs (unloaded micelles) for 48h. Results shown are the mean ± SD of at least two experiments done with six replicates each.

RADIOLABELED MICELLES

In order to verify if the radioactive compound was encapsulated inside the micelles, it was necessary to measure the activity of the solutions after the centrifugation: filtered and the recovered solution from the filter (solution with the micelles), and also the activity adsorbed to the filter. The results can be found on the Table 5.

Table 5 – Activity of Radiolabeled BCMs.

		Activity (µCi)	Efficiency (%)
^{111}In-BCMs	**Filtered**	4.57	86.79
	Filter	13.6	
	Recovered from the Filter	119.4	
^{67}Ga-BCMs	**Filtered**	144	73.95
	Filter	114.5	
	Recovered from the Filter	734	

As expected, the activity of the solution recovered from the filter (radiolabeled micelles) is higher when compared to the activity of the filtrate, which indicates that most of the quantity of the radioactive oxine (^{67}Ga-oxine or ^{111}In-oxine) were encapsulated into the micelles. In addition, it is important to mention that the activity adsorbed to the filter can be neglected – activities are very low when compared to the ones of the recovered solution from the filter – meaning that the radioactive compounds are not significantly adsorbed by the filter. Also, the efficiency of labelling was calculated and as it possible to observe the values are high (> 73% for ^{67}Ga and > 86% for ^{111}In).

After purification by the Amicon filters, the radiolabeled micelles loaded with ^{67}Ga-oxine or ^{111}In-oxine (^{67}Ga-BCMs and ^{111}In-BCMs) were obtained with high purity (> 95% activity retained in the micelles for both cases).

Recently, a similar methodology was described for radiolabeling polymeric micelles using ^{111}In-tropolone to be incorporated into the micelles core.[26] However, the authors reported a lower radiolabeling yield of the micelles (34 ± 1%) in comparison to the radiolabeling yield observed by us, for ^{67}Ga-BCMs (73.9 %) and specially for ^{111}In-BCMs (86.8%).

The *in vitro* stability of radiolabeled micelles was studied for 6 days (^{111}In-BCMs) and 4 days (^{67}Ga-BCMs) at 37°C by incubation with 0.1 M PBS buffer pH 7.4 (physiological conditions) and the results are shown in Table

6. The release of radioactivity was measured as an indicator for the stability of the ^{67}Ga-oxine or ^{111}In-oxine-labeled micelles. To evaluate the release of the radioactivity from the micelles, the solutions incubated in physiological conditions were filtrated by centrifugation with Amicon filters. The activity released from the micelles was in the filtrate while the activity retained in the filter represents the activity retained inside the micelles. The activity was measured and used to calculate the % of activity inside the micelles (Table 6).

Table 6 – *In vitro* Stability of Radiolabeled micelles.

	t (days)	Act. Filtered (µCi)	Act. Recovered Solution (µCi)	(%)
^{111}In-BCMs	2	0.35	19.84	98.27
	6	0.13	4.06	96.90
^{67}Ga-BCMs	4	0.27	6.08	95.83

Once again, the activity of the recovered solution is higher when compared to the one of the filtered, so it is possible to conclude that the radiolabeled micelles are stable. The lower activity has to do with the isotope decay.

3.1 BIODISTRIBUTION

In order to have preliminary data concerning the pharmacokinetics of the radiolabeled micelles, the biodistribution was studied at 4 h and 24 h after administration. Biodistribution is influenced by the interactions of the micelles with the organs, which are dependent on the physical and biochemical properties of the micelles and the characteristics of the organs[12]. Once the nanocarriers are injected, they are transferred by the bloodstream and distributed to peripheral organs, and simultaneously cleared by these organs. The clearance can be hepatic (through liver), renal (through kidneys), gastric (through gastrointestinal track) or mucociliary (through lungs), depending on the properties of nanoparticles[12,13].

The biodistribution was done for the ^{67}Ga labelled micelles (^{67}Ga-BCMs) and the data obtained from the study are shown in Figure 5.

The uptake in the tissues was determined and presented as a percentage of the injected activity per gram of organ/tissue. (% I.A./g ± SD). The whole-body radioactivity excretion was determined as a percentage of the total injected activity. A relatively slow blood clearance was observed, with values of 7.3 ± 1.3 and 2.6 ± 1.3 % I.A./g blood at 4 h and 24 h post-injection (p.i.),respectively, and it is in accordance with the behaviour previously observed for micelles radiolabeled with ^{188}Re (11.2 ± 0.9 and 4.6 ± 1.5 % I.A./g blood at 4 h and 24 h p.i., respectively)[27]. Radioactivity accumulation detected in highly irrigated organs such as lungs and heart may be attributed to the high activity in the blood pool with slow washout from these organs that clear over time.

After the 4 h p.i., a relevant liver uptake was found (10.9 ± 0.4 %I.A./g organ) that decreased at 24 h p.i. (5.5 ± 1.1 % I.A./g organ), which indicates that the main route of clearance is the hepatobiliary excretory pathway. Although, some significant kidney uptake was also observed (7.5 ± 0.5 I.A./g at 4 h p.i.), that was mostly retained at 24 h (4.7 ± 0.8% I.A./g), also suggesting the involvement of renal elimination.

The bone uptake (femur) increased after 24 h p.i. (6.8 ± 1.0 %I.A./g organ at 4h to 9.4 ± 1.3 %I.A./g organ) which can mean that there is free ^{67}Ga inside the body, since in previous studies[28] the uptake of free gallium-67 by the bone increased after 24 h p.i..

In addition, the rate of radioactivity excretion was low: 9.5 ± 2.4 %I.A. after 4 h p.i. and 30.6 ± 2.2 %I.A. after 24 h p.i.. This behaviour agrees with the expected distribution profile in micelle formulations.

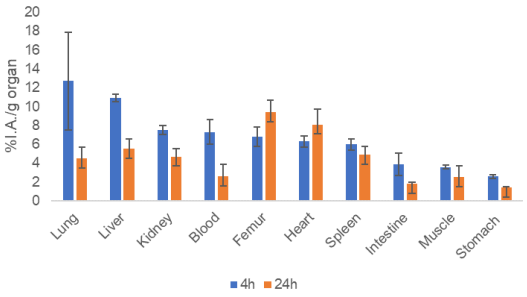

Figure 5 – Biodistribution of ^{67}Ga-BCMs micelles in CD1 health mice at 4 h and 24 h p.i., expressed as %I.A./g organ**.**

4 CONCLUSIONS

The BCMs-Au(cdc)$_2$ chosen were the AS6 (the solvent used for dissolution was chloroform and the one used for the hydration of the thin-film was water, 50 mg of polymer and 2 mg of [Au(cdc)$_2$]$^-$) since the loading efficiency was 64.59% and the loading content of 35.29 mg$_{[Au(cdc)2]}$-/g$_{BCM}$. The loading content was compared to a previous study with auranofin, which LC was 1.8 – 6.2 mg. These results show a drug loading content higher in the [Au(cdc)$_2$]$^-$ loaded micelles, indicating that [Au(cdc)$_2$]$^-$ is encapsulated more efficiently using the optimized formulation. This is a very important achievement since a lower quantity of loaded micelles may be used to deliver the same amount of gold complex.

The chosen micelles had a hydrodynamic diameter of 77.31 ± 27.00 nm and since the d_h of polymeric micelles can vary between 10 – 100 nm, micelles were formed. In addition, the sample had a PdI of 0.18, meaning that the sample was homogenous and polymeric micelles are acceptable as drug delivery carriers. Also, the surface of the micelles was negatively charged (zeta potential of -57.20 ± 12.10 mV), which means that the rate of clearance from the blood is high what can be a problem since micelles have to remain in circulation for longer intervals without being taken up by the MPS in order to enter the tumour tissues through the EPR effect. Besides that, the absolute value of Z_p (=57.20 ± 12.10 mV), suggests high stability of the micelles

Cytotoxic activity studies against the ovarian A2780 cancer cells, have shown that [Au(cdc)$_2$]-loaded BCMs maintain relevant cytotoxic activity comparable to the cytotoxicity observed for the same concentration of gold complex.

The last part of the experiment was the formation of radiolabeled micelles using ^{111}In and ^{67}Ga as isotopes, which was done by the encapsulation of the radioactive compounds inside the micelles, and the study of the biodistribution of ^{67}Ga-BCMs. The efficiency of labelling was high (> 70%), when compared to previous studies, whose efficiency achieved was only 34 ± 1% for ^{111}In[26]. After the biodistribution study, it was possible to conclude that the radioactivity accumulation was detected in highly irrigated organs such as lungs and heart which may be attributed to the high activity in the blood pool with slow washout from these organs that clear over time. In addition, after 24 hours post-injection it occurred bone uptake, which can mean that there was free gallium-67 inside the mice. Most importantly, this preliminary biodistribution study has shown a prolonged circulation lifetime in the bloodstream, suggesting that the micelles are potentially useful as drug delivery to tumours exploring the EPR effect.

5 REFERENCES

1. Khalid M. El-Say & Hossam S.El-Sawy. Polymeric nanoparticles: Promising platform for drug delivery. *Int. J. Pharm.* **528**, 675–691 (2017).

2. Jong, W. H. De & Paul, J. B. Drug delivery and nanoparticles : Applications and hazards. *Int. J. Nanomedicine* **3**, 133–149 (2008).

3. Jhaveri, A. M. & Torchilin, V. P. Multifunctional polymeric micelles for delivery of drugs and siRNA. *Front. Pharmacol.* **5 APR**, 1–26 (2014).

4. Cabral, H., Miyata, K., Osada, K. & Kataoka, K. Block Copolymer Micelles in Nanomedicine Applications. *Chem. Rev.* **118**, 6844–6892 (2018).

5. Lamberti, M., Zappavigna, S., Sannolo, N., Porto, S. & Caraglia, M. Advantages and risks of nanotechnologies in cancer patients and occupationally exposed workers. *Expert Opin. Drug Deliv.* **11**, 1087–1101 (2014).

6. Oerlemans, C. *et al.* Polymeric micelles in anticancer therapy: Targeting, imaging and triggered release. *Pharm. Res.* **27**, 2569–2589 (2010).

7. Yadav, H. K. S., Almokdad, A. A., shaluf, S. I. M. & Debe, M. S. *Polymer-Based Nanomaterials for Drug-Delivery Carriers*. *Nanocarriers for Drug Delivery* (Elsevier Inc., 2019). doi:10.1016/b978-0-12-814033-8.00017-5.

8. Amin, M. C. I. M., Butt, A. M., Amjad, M. W. & Kesharwani, P. *Polymeric Micelles for Drug Targeting and Delivery*. *Nanotechnology-Based Approaches for Targeting and Delivery of Drugs and Genes* (Elsevier Inc., 2017). doi:10.1016/B978-0-12-809717-

5.00006-3.

9. Rizvi, S. A. A. & Saleh, A. M. Applications of nanoparticle systems in drug delivery technology. *Saudi Pharm. J.* **26**, 64–70 (2018).

10. Kumar, R., Kulkarni, A., Nagesha, D. K. & Sridhar, S. In vitro evaluation of theranostic polymeric micelles for imaging and drug delivery in cancer. *Theranostics* **2**, 714–722 (2012).

11. Zhou, Q., Zhang, L., Yang, T. H. & Wu, H. Stimuli-responsive polymeric micelles for drug delivery and cancer therapy. *Int. J. Nanomedicine* **13**, 2921–2942 (2018).

12. Wei, Y., Quan, L., Zhou, C. & Zhan, Q. Factors relating to the biodistribution & clearance of nanoparticles & their effects on in vivo application. *Nanomedicine* **13**, 1495–1512 (2018).

13. Bourquin, J. *et al.* Biodistribution, Clearance, and Long-Term Fate of Clinically Relevant Nanomaterials. *Adv. Mater.* **30**, 1–31 (2018).

14. Pricker, S. P. Medical uses of gold compounds: Past, present and future. *Gold Bull.* **29**, 53–60 (1996).

15. Cholkar, K., Patel, A., Dutt Vadlapudi, A. & K. Mitra, A. Novel Nanomicellar Formulation Approaches for Anterior and Posterior Segment Ocular Drug Delivery. *Recent Patents Nanomedicinee* **2**, 82–95 (2012).

16. Xie, X. *et al.* Challenges and Opportunities from Basic Cancer Biology for Nanomedicine for Targeted Drug Delivery. *Curr. Cancer Drug Targets* **19**, 257–276 (2019).

17. Khodabandehloo, H., Zahednasab, H. & Hafez, A. A. Nanocarriers usage for drug delivery in cancer therapy. *Int. J. Cancer Manag.* **9**, (2016).

18. Ribeiro, E. *et al.* Radiolabeled block copolymer micelles for image-guided drug delivery. *Int. J. Pharm.* **515**, 692–701 (2016).

19. Sousa, S. A. *et al.* On the path to gold: Monoanionic Au bisdithiolate complexes with antimicrobial and antitumor activities. *J. Inorg. Biochem.* **202**, 110904 (2020).

20. Retention Time. https://www.sciencedirect.com/topics/chemistry/retention-time.

21. Díez-Martínez, R. *et al.* Auranofin-loaded nanoparticles as a new therapeutic tool to fight streptococcal infections. *Sci. Rep.* **6**, 19525 (2016).

22. Polymeric Micelle. https://www.sciencedirect.com/topics/engineering/polymeric-micelle.

23. Danaei, M. *et al.* Impact of Particle Size and Polydispersity Index on the Clinical Applications of Lipidic Nanocarrier Systems. *Pharmaceutics* **10**, 57 (2018).

24. Smith, M. C., Crist, R. M., Clogston, J. D. & McNeil, S. E. Zeta potential: a case study of cationic, anionic, and neutral liposomes. *Anal. Bioanal. Chem.* **409**, 5779–5787 (2017).

25. Raza, K., Kumar, P., Kumar, N. & Malik, R. Pharmacokinetics and biodistribution of the nanoparticles. *Adv. Nanomedicine Deliv. Ther. Nucleic Acids* 166–186 (2017) doi:10.1016/B978-0-08-100557-6.00009-2.

26. Laan, A. C. *et al.* Radiolabeling polymeric micelles for in vivo evaluation: a novel, fast, and facile method. *EJNMMI Res.* **6**, 1–10 (2016).

27. Ribeiro, E. *et al.* Docetaxel-loaded block copolymer micelles labeled with 188Re for combined radiochemotherapy. *J. Drug Deliv. Sci. Technol.* **60**, 101898 (2020).

28. Fazaeli, Y. *et al.* Development of ga-67 maltolate complex as an imaging agent. *Iran. J. Pharm. Res. IJPR* **11**, 755–62 (2012).